Aspects of Molecular Medicine 3 (2024) 100039

Contents lists available at ScienceDirect

Aspects of Molecular Medicine

journal homepage: www.journals.elsevier.com/aspects-of-molecular-medicine

A canine mastocytoma with oncogenic c-kit activation by intra-exonic alternative splicing

Mengrui Li [a,b], Stephanie Vanegas [a], Mia R. Gonzalgo [a], Joseph A. Lacret [c], Wensi Tao [d], Sapna Deo [a,b,e], Sylvia Daunert [a,b,e,**], Jean-Marc Zingg [a,b,*]

[a] Department of Biochemistry and Molecular Biology, Miller School of Medicine, University of Miami, Miami, FL, 33136-6129, USA
[b] Dr. JT Macdonald Foundation Biomedical Nanotechnology Institute, University of Miami, Miami, FL, 33136, USA
[c] Red Bird Animal Clinic, Coral Gables, FL 33155, USA
[d] Department of Radiation Oncology, University of Miami-Miller School of Medicine, Miami, FL, 33136, USA
[e] University of Miami Clinical and Translational Science Institute, University of Miami, Miami, FL, 33136, USA

ARTICLE INFO

Handling editor: A Angelo Azzi

Keywords:
Mastocytoma
Gastrointestinal stromal tumor
C-kit
Alternative splicing
Hyperthermia
Evolution
Intron retention
Heat stress

ABSTRACT

We report a subcutaneous mastocytoma in a mid-aged Italian greyhound dog with a small 41 bp genomic deletion of the c-kit gene leading to skipping of the authentic 3′-splice junction of intron 10. The shift to an alternative splice junction in exon 11 leads to a mis-spliced in-frame mRNA transcript with a 27 bp deletion of exon 11 coding for 9 amino acids in the juxtamembrane negative regulatory domain of c-kit tyrosine kinase. In the tumor, c-kit was activated as revealed by more pronounced c-kit-regulated signaling by the PI3K/Akt and G-coupled receptor pathways. The same 9 amino acids deletion was reported in several human gastrointestinal stromal tumors (GIST) pointing to a remarkable similarity of c-kit activation by small deletions and aberrant splicing in humans and dogs, independent of exact sequence context, tumor type and location. Interestingly, the alternative splice junction in exon 11 has been conserved in *Primates* but less in other *Orders* with increased body temperature such as ruminants. We hypothesize that elevated body temperature has acted as evolutionary pressure to eliminate the alternative splice site at this hotspot. At a molecular level, hyperthermia may increase the frequency of small deletions in the c-kit gene by facilitating base slipping or hindering repair. An RT-qPCR assay was developed to detect c-kit alternative splicing in tumors and cell lines exposed to hyperthermia. The molecular mechanisms of tumorigenesis are discussed.

1. Introduction

Cutaneous mastocytoma is a common mesenchymal tumor in dogs, and it occurs more frequently in certain dog breeds such as Boston terrier, Boxers, Labradors and Golden retrievers. The incidence increases with age, starting at around 6 years of age (which is the human equivalent of 40 years). Comparative oncology has established that the disease symptoms are strikingly similar in dogs and man, and unraveling the oncogenic mechanisms of canine mastocytomas may benefit other species such as humans, cats, mice and oxen in which mastocytomas occur much less frequently (Orkin, 1967; Willmann et al., 2019; de Nardi et al., 2022). Accordingly, canine lymphoma models have been instructive for understanding the etiology and to develop treatments of human non-Hodgkin's lymphoma (Richards and Suter, 2015; Ito et al., 2014).

In canine mastocytoma, gain of function mutations of the extracellular domain of the c-kit receptor as well as the intracellular tyrosine kinase domain have been frequently identified (Letard et al., 2008). These mutations lead to constitutive activation of c-kit tyrosine kinase activity as result of auto-phosphorylation. Activating c-kit mutations in canine mastocytomas are often found in exons 8–11. The usual treatment of canine mastocytoma is surgical excision of the cutaneous nodules, and systemic administration of corticosteroids (Willmann et al., 2021). For therapy, constitutive activation of c-kit can be inhibited by a number of tyrosine kinase inhibitors (TKI) (Willmann et al., 2019; Hadzijusufovic et al., 2012). Adjuvant treatments commonly include chemotherapy with prednisone, vincristine, vinblastine, lomustine, or multidrug protocols and radiation therapy (Spugnini et al., 2011).

* Corresponding author. Department of Biochemistry and Molecular Biology, Miller School of Medicine, University of Miami, Miami, FL, 33136-6129, USA
** Corresponding author. Department of Biochemistry and Molecular Biology, Miller School of Medicine, University of Miami, Miami, FL, 33136-6129, USA.
E-mail addresses: sdaunert@med.miami.edu (S. Daunert), jaz42@miami.edu (J.-M. Zingg).

https://doi.org/10.1016/j.amolm.2024.100039
Received 5 February 2024; Received in revised form 22 March 2024; Accepted 24 March 2024
Available online 27 March 2024

However, radiation and chemotherapy always result in high immune responses and long-term side effects. Some success was observed in dogs with mastocytoma by treatment with vitamin E analogues such as δ-tocotrienol that prevented recurrence (Olivieri, 2020). Possible mechanisms by which proliferation of mast cell tumor cells are reduced by vitamin E analogues may involve inhibition of Akt/PKB activity that is activated by c-kit (Kempna et al., 2004). Vitamin E analogues may also help in suppressing degranulation of mast cells (Gueck et al., 2002; Tsuduki et al., 2013; Zingg, 2007). A recent case report on a dog with mastocytoma showed success by changing to a ketogenic diet, again most likely as result of inhibition of Akt/PKB (Robey and Hay, 2009; Kumar et al., 2021; Seyfried et al., 2023).

In humans, cutaneous mastocytoma occur mostly in childhood, approximately 40% of children have exon 17 c-kit mutations, another 40% have c-kit mutations outside exon 17 (e.g., exon 8, 9, 10, 11), and the remaining have no detectable c-kit mutations (Leung et al., 2019). In humans, advanced mast cell neoplasms are rare with poor prognosis and limited treatment options and only few preclinical models, whereas in dogs they are the most frequent malignant skin tumors (Willmann et al., 2019). Other tumors in humans having c-kit mutations include gastrointestinal stromal tumor (GIST) originating from interstitial cells of Cajal, melanoma, cutaneous melanoma, lung adenocarcinoma, and anorectal melanoma. C-kit exon 11 mutations are present in 0.85% of American Association of Cancer Research Genomics Evidence Neoplasia Information Exchange (AACR GENIE) cases, and most oncogenic gain of function mutations in GIST affect the juxtamembrane domain of exon 11 (Lasota et al., 1999; Corless et al., 2004; Chen et al., 2005; Consortium, 2017).

Here we analyzed a recurring subcutaneous mastocytoma in a mid-aged Italian greyhound dog and detected a deletion in the c-kit gene at the intron 10/exon 11 junction. The deletion leads to oncogenic activation of c-kit by alternative splicing to a novel 3′-splice site within exon 11, similar to what has been reported for human GIST (Lasota et al., 1999; Corless et al., 2004; Chen et al., 2005; Incorvaia et al., 2021). These findings point to a remarkable similarity of c-kit activation by small deletions and alternative splicing in humans and dogs, independent of tumor type and location. Interestingly, the alternative splice junction in exon 11 is mostly absent in ruminants and other species that can have a higher body temperature, suggesting that hyperthermia may act as evolutionary pressure to eliminate it. At the mechanistic level, the genomic instability generated by hyperthermia may increase the risk for small deletions. An RT-qPCR assay was developed for detecting tumor cells with alternative splicing of c-kit and facilitates early detection of this cancer after biopsy in a minimally invasive manner. The analysis of the mechanisms by which tumors arise in humans and dogs by comparative molecular oncology may help in accelerating diagnosis, prognosis and novel therapy (Willmann et al., 2019).

2. Materials and methods

2.1. Pathologic assessment of tumor tissue

The patient, an 8-year-old Italian greyhound, presented to Red Bird Animal Clinic, Coral Gables, Florida, USA with recurring dorsal mastocytoma, stage 1. The excised nodule was round shaped (1.5 cm^3) with a soft consistency, and mast cell tumor was suspected by cytology. The microscopic interpretation of the skin nodule was subcutaneous mast cell tumor (SCMCT). Mitotic count: 0 per 2.4 mm^2 (equivalent to ten 400x high power fields (HPF)). Excision of this mass appeared incomplete, with neoplastic cells extending to lateral and deep margins. No lymphatic/vascular invasion was observed, and no further treatment was required. SCMCTs are located exclusively within the subcutis or may also mildly extend into the overlying deep dermis. More than 90% of SCMCTs are controlled by surgical excision alone, and it is important to distinguish SCMCTs from cutaneous mast cell tumors (CMCTs), which are located within the dermis, with/without involvement of the underlying subcutis (Thompson et al., 2011a, 2011b). However, 10% of dogs with SCMCT die of MCT-related disease, 11% develop a second SCMCT distant from the primary site, 8% recur, and 5% metastasize (Kiupel and Camus, 2019). In this study only discarded samples from spontaneous disease were used. All procedures followed a high standard (best practice) of veterinary care, and an informed consent statement was given by the client/owner. Based on the finding that vitamin E analogues can inhibit c-kit-activated Akt/PKB and recurrence of canine mastocytoma, the patient (~25 kg body weight) was given one capsule of Annatto per day (125 mg tocotrienols, TT), 90% δ-TT, 10% γ-TT (Wellness extract, USA)) as well as 25 mg/day Benadryl minitablet (Rite Aid) for one year and had no relapse (Olivieri, 2020; Kempna et al., 2004). For mast cell tumors, the histamine receptor 1 antagonist Benadryl (diphenhydramine HCl) may reduce tumor cell proliferation and help mitigate mediator-related clinical symptoms resulting from activated mast cells (Gamperl et al., 2021). Some further lesions appeared (lipoma in sternum, leg), but analysis did not show the presence of the exon 11 deletions, suggesting no metastatic origin.

2.2. Isolation of total RNA and genomic DNA

Tumor and surrounding normal tissue were soaked in RNAlater (Qiagen) and stored at −80°C. Small pieces were cut out, homogenized with a tissue homogenizer (T10 basic Ultra-TURRAX, IKA) in QIAzol lysis solution and total RNA was isolated using a RNeasy Plus Universal mini kit (Qiagen). cDNA was synthesized using a High-capacity cDNA reverse transcription kit (Applied Biosystems). Total genomic DNA from normal and tumor tissue was isolated using the Wizard genomic DNA purification kit (Promega).

2.3. DNA amplification

PCR for cDNAs was performed using Q5 High-Fidelity DNA polymerase (NEB) with exon 8/11 and 11/13 primers (Table 1), and 30s 98°C pre-heating, 10s 98°C, 30s 45–55°C, 2 min 72°C, 4 min 72°C for 40 cycles. PCR for genomic DNA was performed using Q5 High-Fidelity DNA polymerase (NEB) with intron 10/11 primers (Table 1) and 30s 98°C pre-heating, 10s 98°C, 10s 60°C, 10s 72°C, 4 min 72°C for 40 cycles. Amplified PCR products were separated by 1.5–2.5% agarose gels

Table 1
Primers used in this study.

Primers	5′-3′- sequence
Exons 8/11	
8f (Exon8fw) (Letard et al., 2008)	GGGAACGAAGGAGGCACTTACACA
11r (Exon11rv) (Letard et al., 2008)	CATCCGACTTAATCAGGCCATA
Exons 11/13	
11f (Exon11fw) (Letard et al., 2008)	ATGTATGAAGTACAGTGGAAGG
13r (Exon13rv) (Letard et al., 2008)	AAGTGCCACTTCTCCGTGATC
Exons 10/11	
Ckitfw (canine)	CTGGAATGATGTGCATTATCGT
Ckitrv (canine)	AGGAAGCTGTGTTGGGTCTATG
Hkitfw (human)	CTGGCATGATGTGCATTATTGT
Hkitrv (human)	AGGAAGTTGTGTTGGGTCTATG
Intron 10/11	
Ckitfw (canine)	CTGGAATGATGTGCATTATCGT
Ckitrv (canine)	AGGAAGCTGTGTTGGGTCTATG
Taqman probes	
HKitnorm (human)	FAM-TGAAGTACAGTGGAAGGTTGTTGAGGAG
HKittum (human)	VIC-**AC**AGGTTGTTGAGGAGATAAATGGA
HKittum1 (human)	VIC-**TAC**AGGTTGTTGAGGAGATAAATGG
Hkit 9/11	
H9f	CCACCGTTTGGAAAGCTAGTG
H10/11delrv (deleted)	ATTTATCTCCTCAACAACCTGT
H10/11wtrv (normal)	ATTTATCTCCTCAACAACCTTC

and the bands extracted using a gel extraction kit (Qiagen) and sequenced (Genewiz). Sequence analysis was done using NBlast (NCBI).

2.4. RNAseq analysis

Total RNA from three samples was isolated from tumor and adjacent normal tissue as described above. The RNA was analyzed by RNAseq and differential gene expression and gene ontology enrichment evaluated (n = 3) (Novogene, Co., Ltd).

2.5. Growth of cells and heat treatment

Human erythroleukemia cells (HEL, TIB-180, ATCC) were grown in DMEM/10% FCS, 100 µg/ml streptomycin, and 100 U penicillin. Cell numbers were determined using a Moxi miniautomated cell counter (Orflo). Three test groups were made: group #1 cultured at 37 °C full time without heating, group #2 cultured at 37 °C with 2 h heating at 40 °C once a week, group #3 cultured at 37 °C with 2 h heating at 42 °C once a week. A new cell passage was made by 1/10 dilution once a week. In a second series of experiments HEL cells were grown with reduced serum in DMEM/0.2% FCS, 100 µg/ml streptomycin, and 100 U penicillin. Two additional test groups made from group #2 and #3 in 0.2% FCS; group #1A cultured at 37 °C with 2 h heating at 40 °C once a week, and group #2A cultured at 37 °C with 2 h heating at 42 °C once a week. A new cell passage was made by 1/10 dilution once a week (Fig. S1A). Cells were harvested and $2x10^6$ cells used to prepare total RNA as described above. Total cell numbers that were harvested each week were used to determine cumulative cell numbers and plotted (Figs. S1B and C).

2.6. Development of RT-qPCR assay for detection of exon 11 deletion

Total RNA was extracted from normal and tumor tissue, and from the different groups of HEL cells grown as described above. cDNA was synthesized using a High-capacity cDNA reverse transcription kit (Applied Biosystems) and used for the RT-qPCR assay. Specific Taqman probes were developed using the PrimerQuest tool (Integrated DNA Technology (IDT)) (Table 1) that overlap with the site of the deletion at the exon10/11 junction. Single-tube amplification conditions were optimized so that the FAM-labeled Taqman probe HKitnorm for normal tissue binds only to the normal amplicons, whereas the VIC-labeled Taqman probe HKittum1 for the tumor tissue binds only to the alternatively spliced tumor amplicons and can distinguish cDNA in which the deletion is present (tumor) from cDNA in which it is absent (normal). RT-qPCR assay for cDNAs was performed using Q5 High-Fidelity DNA polymerase (NEB) with CKitfw and CKitrv primers for canine samples in the presence of these Taqman probes (Table 1), with optimized conditions as 30s 98°C pre-heating, 10s 98°C, 30s 65°C, 2 min 72°C, 4 min 72°C for 40 cycles. For samples from human HEL cells, HKitfw and HKitrv primers were used for amplification, and reactions were run in separate tubes for normal HKitnorm and tumor HKittum1 Taqman probes. GAPDH was used as internal control.

2.7. Statistical analysis

All experiments were done at least in duplicate. Values are expressed as the mean ± standard error of the mean (SEM) as explained in the figure legends.

3. Results

3.1. Identification of a 27 bp cDNA deletion in c-kit exon 11

A tumor was detected in the hindquarters of a mid-aged Italian greyhound dog and pathologically characterized as subcutaneous mastocytoma. Total RNA from tumor and adjacent normal tissue was reverse transcribed and the cDNA analyzed by amplifying the c-kit gene known to be frequently mutated in canine mastocytoma. A 27 bp deletion of the c-kit exon 11 was detected only in the tumor tissue coding for 9 amino acids in the juxtamembrane negative regulatory domain of c-kit tyrosine kinase (Fig. 1). The 5′-end of the 27 bp deletion corresponded to the 5′-end of exon 11 so that it was suspected to be the result of a small deletion at the intron10/exon11 junction. Alternatively, since in exon 11 an alternative splice site was detected, it appeared also possible that it originated from alternative splicing.

3.2. Identification of a genomic 41 bp deletion in c-kit overlapping the intron 10/exon 11 junction

Total genomic DNA from normal and adjacent tumor tissue was isolated, and a region of the c-kit gene spanning exon 10 – exon 11 was amplified and sequenced. In the tumor a small 41 bp genomic deletion of the c-kit gene was detected at the intron10/exon11 junction leading to skipping of the authentic 3′-splice junction of intron 10 and usage of the alternative splice site in exon 11 (Fig. 2). In the genomic DNA from the adjacent normal tissue the deletion was absent.

3.3. Alternative splice site selection as result of a genomic deletion

Alignment of the canine and human genomic DNA sequence of the exon10/intron10/exon 11 revealed that the exon sequences are highly conserved, the exon/intron junction and branch point are at the same place, whereas the intron sequence is variable (Fig. 3). Interestingly, the same 9 amino acids of exon 11 were reported to be deleted in several human gastrointestinal stromal tumors (GIST), that were also the consequence of similar small deletions at the intron 10/exon 11 junction (US patent 9260525B2) (Lasota et al., 1999; Corless et al., 2004; Chen et al., 2005; Incorvaia et al., 2021). Similar clinical short variants <50 bp at the c-kit intron 10/exon 11 junction have been reported in several other clinical human tumors (Fig. S2). These deletions may possibly be the result of inherent genomic instability at that site leading to polymerase slippage that may be enhanced by mutagens or physical stress such as radiation or heat.

3.4. Intron retention in the tumor

Further, as result of the deletion, a part (11 of the original 18 pyrimidines) of the polypyrimidine tract important for splicing is missing (Fig. 3). In addition, the distance between the pre-mRNA branch point and the authentic and alternative splice sites is different (51 bp versus 37 bp, respectively), what both may lead to less efficient splicing and the presence of unspliced RNA in the tumor (intron retention) (Wong et al., 2017; Monteuuis et al., 2021). Accordingly, amplification of the intron in total RNA showed the retention of unspliced intron 10 only in the tumor but not in the normal tissue indicating inefficient splicing in the tumor and consequent intron retention. In both normal and tumor samples correctly spliced RNA with and without the deletion was detected suggesting that the tumor may have infiltrated into the adjacent normal tissue; whereas the wildtype band was weaker in the tumor sample when compared to the normal sample (Fig. 4).

3.5. Comparison of gene expression in normal and tumor tissue by RNAseq

The shift to an alternative splice junction in exon 11 leads to a mis-spliced in-frame mRNA transcript with a 27 bp deletion of exon 11 and structural analysis showed that the deleted amino acids are coding for 9 amino acids in the juxtamembrane negative regulatory domain of c-kit tyrosine kinase that drives oncogenic signaling and gene expression in the tumor (Chen et al., 2005). RNAseq with total RNA from normal and tumor tissue revealed differential gene expression (Fig. 5a and b). Pathway analysis revealed that genes within the PI3K/Akt pathway and

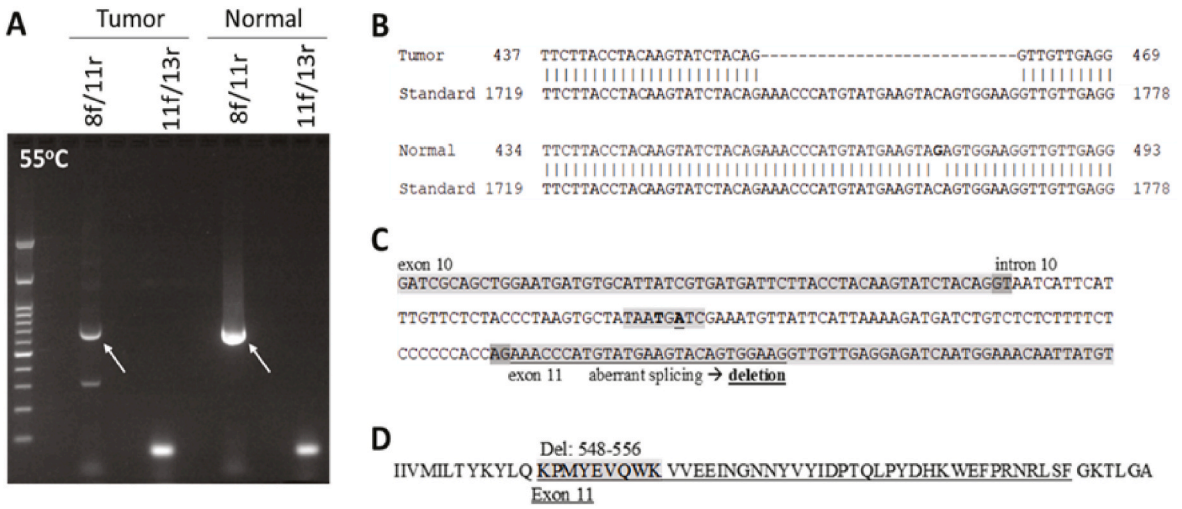

Fig. 1. Detection of c-kit mRNA deletion in exons 8–13 in the tumor tissues. (**A**) Using an annealing temperature of 55°C allows primers 8f/11r to amplify the correct product from cDNA in normal and tumor tissue, but no amplification is observed with primers 11f/13r, possibly because there are polymorphisms/mutation/deletions at the primer binding sites. (**B**) Sequencing reveals aberrant splicing only in the tumor leading to a deletion of 27 bp in the mRNA/cDNA. (**C**) Structure of exon 10, intron 10 and exon 11. **A**: branchpoint in exon 10 (**D**) Deletion of 9 amino acids of the juxtamembrane negative regulatory domain of c-kit tyrosine kinase in exon 11 due to alternative splicing.

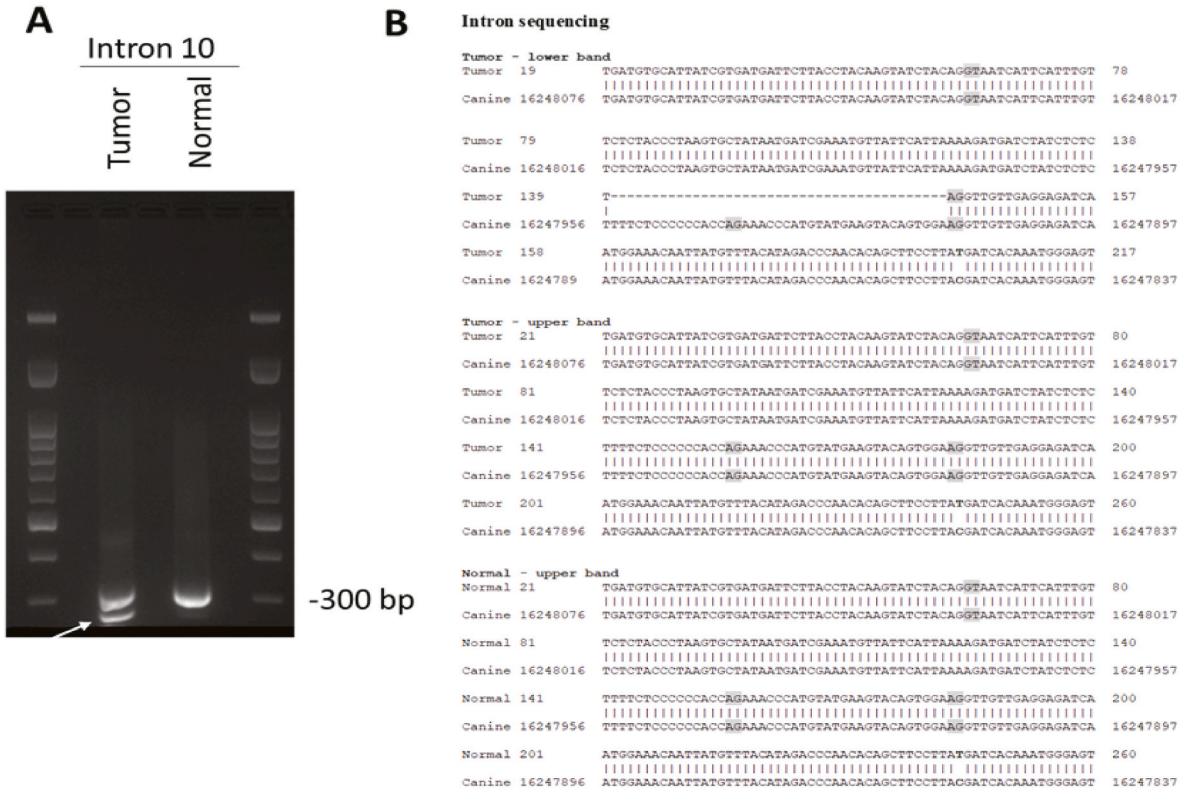

Fig. 2. Detection of a deletion at the intron10-exon11 junction in genomic DNA of tumor tissue. (**A**) PCR amplification of genomic DNA with primers Ckitfw and Ckitrv from normal and tumor tissue, an additional smaller band is visible in the tumor only (arrow). (**B**) The sequence of exons 10, intron 10 and exon 11 reveals a 41 bp deletion at the intron10/exon11 junction. Grey box: splice sites.

the G-coupled receptor pathway are overrepresented in the tumor, in line with the role of activated c-kit in regulating these pathways (Fig. 5c and d).

3.6. Assay development for detection of presence alternative splicing in exon 11 by RT-qPCR

To monitor the presence of a genomic deletion leading to alternative splicing of c-kit exon 11, we developed a sensitive assay based on RT-qPCR (Ruhle et al., 2020). We chose to monitor cDNA/RNA since deletions at the intron 10/exon 11 junction are often variable in size at the

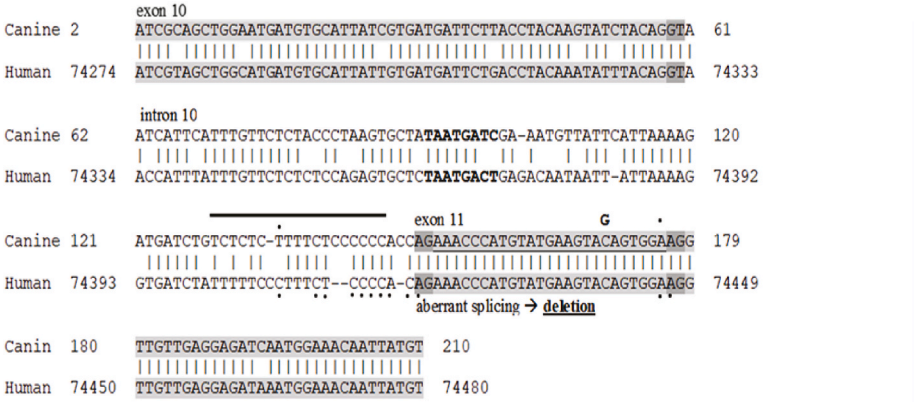

Fig. 3. Comparison of sequences of exon10-intron10-exon11 in humans and dogs. The sequence of exons 10 and 11 of humans and dogs is mostly conserved, including the alternative splice junction in exon 11. Underlined: deletion of exon 11 detected in tumor c-kit cDNA. Overlined: polypyrimidine track in intron 10. Bold: branchpoint consensus sequence in intron 10 (●) Range of extensions reached by the deletions detected in humans with GIST.

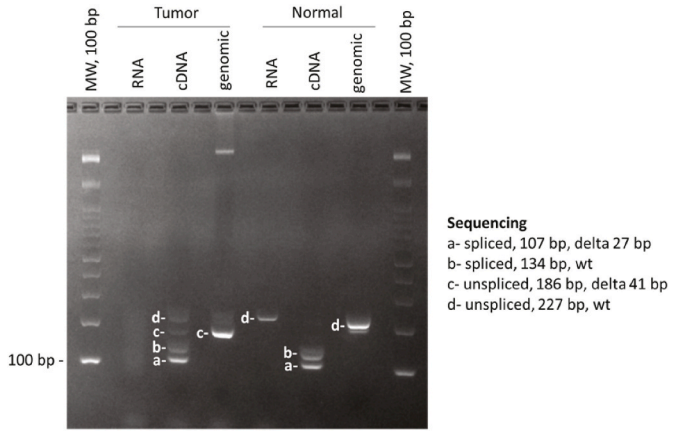

Fig. 4. Intron retention only in tumor. PCR amplification with cDNA isolated from normal and tumor tissue and primers Ckitfw/Ckitrv. In tumors 4 bands representing spliced and unspliced RNA with and without the deletions are detected, whereas in normal cDNA only 2 bands are detected representing spliced wt and tumor RNA. Control genomic DNA gave a smaller fragment in tumor when compared to normal; control RNA did not give a band in tumor but in normal possibly as result of presence of some genomic DNA in the sample.

genomic level, but they all lead to the same 27 bp deletion in exon 11 at the RNA/cDNA level. In this assay total RNA is isolated, cDNA generated and amplified with exon 10 and 11 primers. Single-tube qPCR amplification conditions with the CKitfw and CKitrv primers were optimized so that the FAM-labeled Taqman probe for normal tissue binds only to the normal amplicons, whereas the VIC-labeled Taqman probe for the tumor tissue binds only to the alternatively spliced tumor amplicons (Fig. 6A). The single-tube TaqMan-probe based RT-qPCR assay was able to amplify specifically the wildtype only in the normal and the tumor only in the tumor samples (Fig. 6B).

3.7. Presence of alternative 3′-splice acceptor cite in exon 11 of different species

Sequence alignment of 100 vertebrate species (UCSD genome browser, https://genome.ucsc.edu/) indicated that the authentic 5′-splice junction at exon10/intron10 and the 3′-splice junction at intron10/exon11 are conserved (100%), but the branch point varies (Figs. S3 and S4). When monitoring the presence of the alternative splice site in exon 11 in 100 vertebrate genomes it was not detected in birds, a few fish, marsupials, ruminants, and small vertebrates with desert/tropical habitats suggesting selection against its presence by evolutionary pressures. It appears, that the body and/or egg temperature in the vertebrates that lack the alternative splice site (birds and other descendants from ecto/mesothermic dinosaurs, including alligators), basoendothermic vertebrates (Jerboa, Tenrec), facultative hyperthermic marsupials (Opossum, Platypus, Wallaby, Tasmanian devil), and ruminants, is or can be elevated (close to or above 40°C) (Treat et al., 2018; Lees et al., 2018, 2019; Burnett et al., 2020), leading to the hypothesis that elevated temperature may have been one of the factors leading to elimination of the alternative splice site during evolution.

3.8. Heat-stress may increase the frequency of small deletion

We hypothesized that mild hyperthermia and heat stress may increase the instability of genomic DNA leading to an increased risk for small deletions by facilitating base slipping or hindering repair such as observed in the c-kit intron10/exon11 junction (Amos and Clarke, 2008). The c-kit RNA is strongly expressed in HMC-1 and HEL cells (www.proteinaltas.org) (Fig. S4). We selected human erythroleukemia cells (HEL) as a model system since they grow fast and in suspension and high cumulative cell numbers can be achieved (Molla and Block, 2000). HEL cells were grown at 37°C and subjected once a week to a heat shock at 40°C for 2 h and the total RNA isolated the next day and analyzed for the presence of the small deletion using the developed RT-qPCR assay (Fig. S1). Early passages showed the wildtype c-kit. After growing a total of $3x10^8$ cells using this protocol (passage #17), signals were also obtained with the assay for the alternative splice site but they were very weak (Ct value of ~40). Attempts to increase the signals by growing the cells at 42°C, or by increasing the selective pressure for oncogenic activation of c-kit by reducing the 10% FCS to 0.2% FCS did not improve the signal. Further, the deletion could not be confirmed by sequencing, suggesting that not sufficient mutant cells can be grown with this protocol and an alternative strategy may be required to prove the impact of heat on generating the deletion at this hotspot.

4. Discussion

In this study we identified a small deletion of 41 bp of the c-kit gene in a canine mastocytoma that is identical to one described in human gastrointestinal stromal tumor (GIST) (Lasota et al., 1999; Corless et al., 2004; Chen et al., 2005; Incorvaia et al., 2021). The deletion is located at the junction of intron 10 and exon 11 of the c-kit gene and leads to skipping of the authentic splice site but switching to an alternative splice site in exon 11, leading to a constitutively active c-kit oncogene and overrepresentation of genes regulated by c-kit as analyzed by RNAseq. The presence of an identical small deletion in dogs and humans suggests

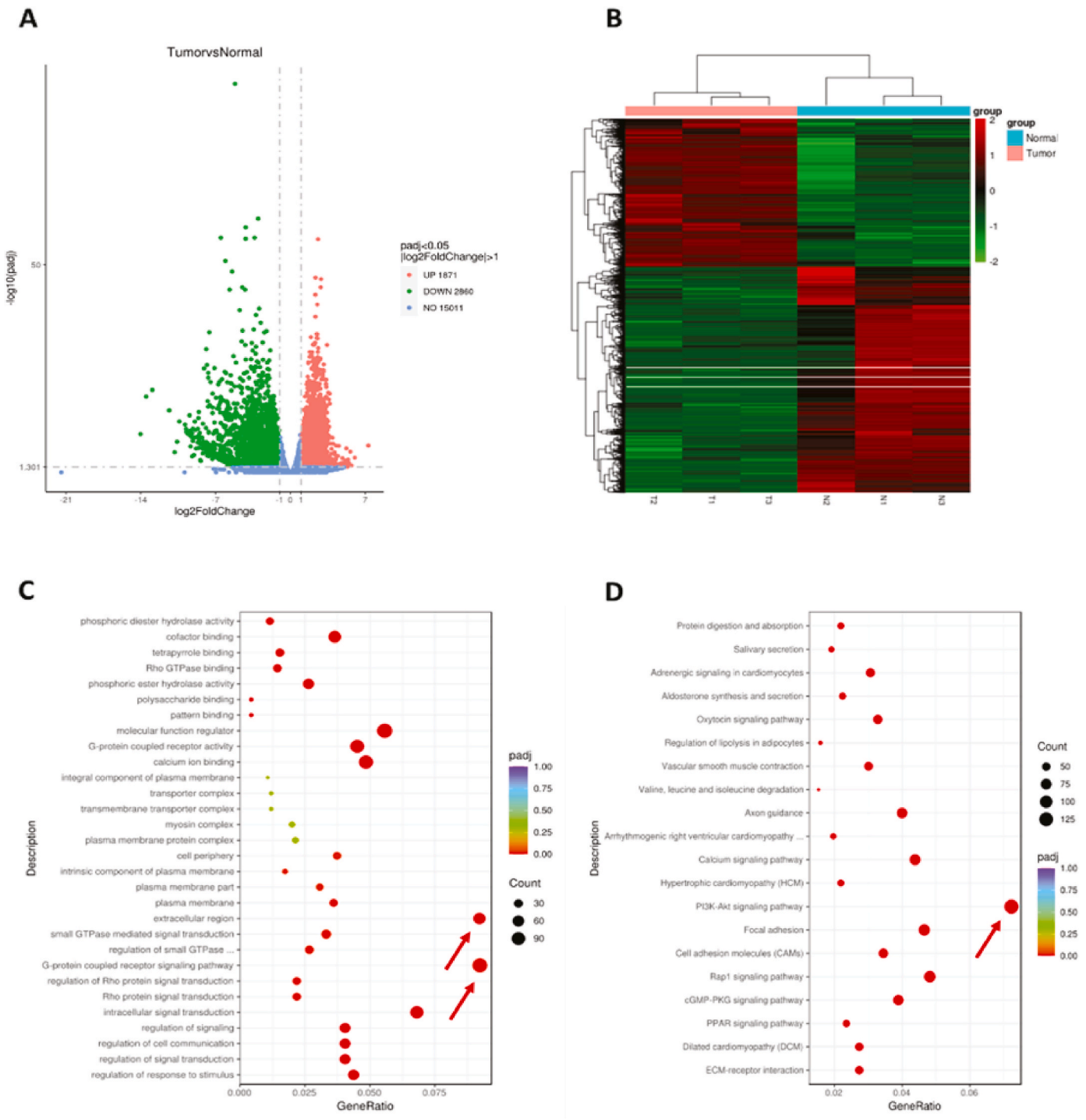

Fig. 5. RNAseq analysis of normal and tumor RNA. (**A**) Differential gene expression, volcano map. (**B**) Differential expression gene clustering heatmap, (**C**) GO enrichment analysis scatter blot; (**D**) KEGG enrichment scatter plot. Arrows: enriched pathways.

common molecular mechanisms by which they are formed, such as mutagens or inherent genomic instabilities at this site. Within the deleted sequence of the canine and human c-kit gene, a stretch of 6 and 4 cytosines, respectively, and homology to a deletion hotspot consensus sequence (TG A/G A/G G/T A/C) may increase the risk of small deletions as reported for the human p53 and other genes (Greenblatt et al., 1996; Krawczak and Cooper, 1991).

Factors that may contribute to the generation of hot spots for small deletion are DNA structure, epigenetic changes, chemical mutagens, UV exposure, defective repair processes, polymerase slippage, or defective splicing factors (Levinson and Gutman, 1987; Wu et al., 2020). In the human genome, mutation hotspots occur by several mutation mechanisms, and short insertion-deletion variations of up to 50 nucleotides (INDEL) are concentrated in about 4% of the genome and occur with a de novo frequency of ~$9x10^{-10}$ per nucleotide per generation (Nesta et al., 2021; Montgomery et al., 2013; Mullaney et al., 2010). Sequence slippage accounts for at least 52% of insertions and 38% of deletions in mammalian genomes (Taylor et al., 2004). Environmental stress, such as cold, heat, hypoxic, and oxidative stresses, can induce instability of long trinucleotide repeats by stimulating DNA rereplication (Chatterjee et al.,

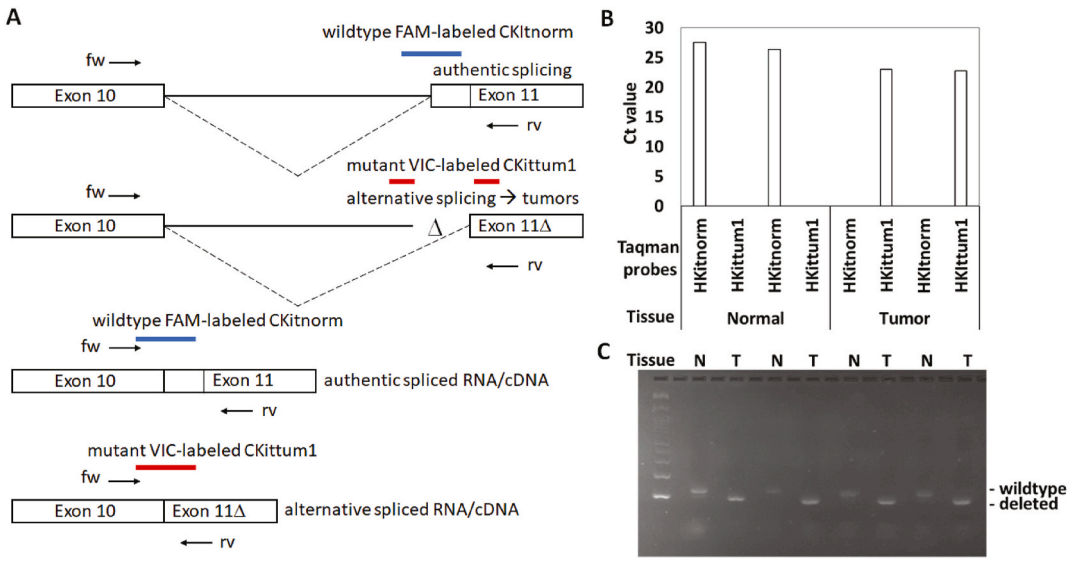

Fig. 6. Development of RT-qPCR assay for detection of exon 11 deletion in tumor tissue and heat-treated cells. (**A**) The presence of the genomic deletion at the intron 10/exon 11 junction leads to activation of an alternative splice junction in exon 11. Authentic spliced normal RNA/cDNA can be distinguished from alternative spliced tumor RNA/cDNA by using a FAM-labeled wildtype or a VIC-labeled mutant Taqman probe during single-tube RT-qPCR. (**B**) Testing Taqman probes CKitnorm and CKittum1 with normal and tumor cDNA samples, Tm 65°C, 20s extension, 40 cycles. Top: Ct values of qPCR, bottom: agarose gel, wildtype 134 bp, deleted 107 bp. (**C**) Agarose gel with amplified products from normal and tumor cDNA with c-kit intron 10/exon 11 deletion samples amplified with primers Ckitfw and Ckitrv.

2015, 2016). High temperature (42°C) can drive topoisomerase mediated chromosomal break repair (Ashour et al., 2021), but at the intron 10/exon 11 junction the consensus sequence of this enzyme is not present (Spitzner and Muller, 1988; Christodoulou et al., 2006). Heat shock might affect DNA integrity both directly and via arrest of replication fork progression (Velichko et al., 2012). Our analysis suggests that hyperthermia may contribute to the increased frequency of small deletions in the c-kit gene by facilitating base slipping or hindering repair.

Repair defects may be caused by denaturation and aggregation of thermolabile proteins and induction of thermotolerance via heat shock proteins (Lepock, 2005; Bettaieb and Averill-Bates, 2015). Hyperthermia can inhibit DNA repair and sensitizes cells to chemotherapeutic agents, with changes observed as low as 40°C (Roti Roti, 2008). Mild hyperthermia induces BRCA2 degradation and inhibits homologous recombination (Krawczyk et al., 2011), whereas BRCA2 also protects mammalian cells from heat shock (Nakagawa et al., 2018). An association of consumption of hot beverages such as tea, coffee, or mate and increased risk of oral and upper gastrointestinal cancer has been reported and drinking very hot beverages was classified as probably carcinogenic to humans (Loomis et al., 2016; Huang et al., 2017; Ernst et al., 2021; Ren et al., 2010). Esophageal cancer risk was found to be increased in the ESCCAPE case-control study by thermal exposure with very-hot beverages (Masukume et al., 2022). In yeast, the mutation rate was increased by hyperthermia (54°C ~ at 60 min) with beverages containing caffeine (Candreva et al., 1993), possibly as result of an increased mutation rate at single-stranded DNA generated at hotspots by heat and inefficient repair (Lin et al., 2021).

To assess whether increased heat may contribute to the generation of the c-kit deletion, we have developed a RT-qPCR assay for detection of the presence of the deletion in tumors. Further, we used this assay to measure the generation of small deletions in the c-kit gene by hyperthermia in cultured human cells. However, after growing $3x10^8$ cells, we could not detect clear presence of the deletion. Thus, to prove that hyperthermia accelerates the formation of the c-kit deletion a higher passage number and selective conditions for the presence of the deletion may be required. We should note that this assay, if further optimized, may be useful in the detection of the c-kit deletion from biopsies, allowing for a minimally invasive diagnosis of this cancer.

Intron retention has been reported in several tumor types (Wong et al., 2017; Monteuuis et al., 2021). We observed that intron retention occurred only in the tumor, and it remains to be investigated whether the shorter polypyrimidine track and non-optimal distance from the alternative splice junction affects the splicing efficiency in the tumor. Alternative splicing in gastric cancer can occur as result of mutation and polymorphisms of *cis*-regulatory splicing factors or of *trans*-acting factors (Li and Yuan, 2017). Interestingly, in humans the splicing enhancers at the authentic normal and alternative spliced tumor sequence were reported to be recognized by different splicing factors, and the presence of only one of the exonic splicing enhancer sequences was sufficient for splicing. These two sites are 100% conserved in the canine sequence: AACCCATGT (nucleotides 2–10 from the 5′ end of exon 11 at the authentic splice site, which is recognized by serine/arginine-rich splicing factor 2 (SRSF2) previously known as SC35, SRp55, and SF2/ASF), or GGTTGTTGAGG (nucleotides 27–37 from the 5′ end of exon 11, at the alternative splice site of the tumor within exon 11, which is recognized by SRSF2 and SRp55) (Chen et al., 2005). Further analysis will be required to assess whether these splicing factors are altered/mutated and affect the genome stability at this site as commonly observed in leukemia, e.g., by strong binding to single-stranded polypyrimidine tracks and interference with repair (Wong et al., 2016, 2017; Monteuuis et al., 2021; Li and Wang, 2021; Lee et al., 2016; Dong and Chen, 2020). The intriguing possibility that the alternative splice site within exon 11 is functional and is used at low frequency or in a regulated manner leading to enhanced c-kit activity remains to be explored.

C-kit or stem cell factor receptor is not only an oncogene with relevance to hematopoietic and gastrointestinal tumors but plays an absolute essential role as receptor for stem cell factor for generation and migration of gametes (oocytes, sperms) and subsequent development of hematopoietic cells (Sette et al., 2000). Inherent instabilities in c-kit are expected to be eliminated during evolution if they interfere with successful reproduction of a species or if they are associated with reduced fitness and cause early disease. When monitoring the presence of this alternative splice site in exon 11 in 100 vertebrate genomes, it was not detected in birds, a few fish, marsupials, ruminants, and small vertebrates with desert/tropical habitats (Jerboa, Tenrec) suggesting selection against its presence by evolutionary pressures. Interestingly, the

body and/or egg temperature in the vertebrates that lack the alternative splice site (birds (and other descendants from ecto/mesothermic dinosaurs, including alligators) (Eagle et al., 2015), basoendothermic vertebrates (Jerboa, Tenrec) (Treat et al., 2018; Oelkrug et al., 2013), facultative hyperthermic marsupials (Opossum, Platypus, Wallaby, Tasmanian devil) (Turner, 2020), and ruminants (Lees et al., 2018, 2019; Burnett et al., 2020) is or can be elevated (close to or above 40°C). Further, it can be speculated that similar to birds the alternative splice site was not present in extinct dinosaurs that can have elevated body temperatures during periods of ovulation as determined by clumped isotope analysis of eggshells (Eagle et al., 2015). In contrast, the vertebrates with the alternative splice site are mostly lactating endothermic vertebrates with a generally stable temperature below 37°C, leading to the hypothesis that elevated temperature may act as one of the evolutionary pressures to eliminate the alternative splice site in exon 11.

In fact, a higher body temperature in mammals has been correlated with maximum microsatellite length and warmer-blooded species have shorter microsatellites (Amos and Clarke, 2008). When monitoring 470 mammals, the alternative splice site in exon 11 is mostly absent in *Artiodactyla*, *Cetartiodactyla*, *Metatheria*, and *Monotremata* (Table S1). Alignment of the 5'-ends of human exon 11 with exon 12 shows that they are related, and the alternative splice junction is conserved (Figure S5). In exon 12, the tendency to remove the alternative splice site is more pronounced, possibly also preventing intra-exonic alternative splicing (Table S2). It is present in most *Primates* (except orangutan, aye-aye, bushbaby, and some lemurs) and less in *Carnivores*. Interestingly, again it is mostly absent in *Cetartiodactyla* and *Artiodactyla* that have in common expansion of the stomach into a multichambered organ (ruminants, whales reflecting their ungulate ancestry), except for deers, kudu and camels (not true ruminants since the chambers are not well defined). Accordingly, it is absent in *Xenarthra* (sloths that have multichambered stomach, but present in ant eaters that do not). It is also absent in all *Afrotheria* and *Metatheria* (except Tasmanian devil) and in *Monotremata*. Overall, it appears that in mammals, during evolution of a larger and multichambered stomach with increased number of interstitial cells of Cajal and mast cells exposed to low pH and hyperthermia, the presence of the alternative splice site became eliminated (Wang et al., 2019).

For dogs with suspected mastocytoma tumors the developed RT-qPCR test may allow the early detection of this cancer after biopsy in a minimally invasive manner. When the reported oncogenic c-kit activation by intra-exonic alternative splicing is present the recurrence progress after surgery can be followed and provide diagnostic assistance for further treatments or additional surgery. For humans, although the precise proportion is disputed, mutations of the c-kit gene are known to be present in over half of GISTs, most commonly in exon 11 which encodes the juxta-membrane regulatory domain (de Silva and Reid, 2003). Whether in biopsies from human GIST and cancers that undergo epithelial-mesenchymal transition (Tang et al., 2014; Wu et al., 2019; Sheikh et al., 2022) the presence of the reported c-kit deletion has any predictive value for malignancy and success of therapy remains to be determined (Taniguchi et al., 1999).

5. Conclusions

Comparative molecular oncology allowed us to gain insights into oncogenic activation of the c-kit gene by alternative splicing in canine mastocytoma and human GIST. With direct and indirect analysis, we propose hyperthermia as potential factor that increases the genomic instability and/or decreases the repair efficiency at this specific site ultimately leading to its elimination in vertebrates with higher body temperature during evolution. Unfortunately, not sufficient cells could be expanded and/or the RT-qPCR assay developed was not sensitive enough to prove that hyperthermia is indeed involved in generating this deletion hotspot. In future studies, more cells could be grown in a bioreactor, or novel assays could be developed that allow enrichment of the deletion by selection. Hyperthermia in conventional animal models (e.g., rodents) can only be imposed transiently but animals with naturally fluctuating body temperature carrying a c-kit transgene with intact intra-exonic alternative splice site could be studied. Measuring the impact of hyperthermia on genome-wide mutation rates and frequency of small deletions is highly relevant not only for humans, but for all species including plants in view of thermal stress as result of increased number of days with extreme temperatures exceeding 40°C globally (Belfield et al., 2021; Jorgensen et al., 2022).

CRediT authorship contribution statement

Mengrui Li: Writing – review & editing, Methodology, Investigation, Formal analysis, Data curation, Conceptualization. **Stephanie Vanegas:** Methodology, Investigation, Formal analysis. **Mia R. Gonzalgo:** Methodology, Investigation, Formal analysis. **Joseph A. Lacret:** Resources, Investigation. **Wensi Tao:** Methodology, Investigation, Formal analysis, Data curation. **Sapna Deo:** Writing – review & editing, Supervision. **Sylvia Daunert:** Writing – review & editing, Writing – original draft, Supervision, Resources, Funding acquisition, Conceptualization. **Jean-Marc Zingg:** Writing – review & editing, Writing – original draft, Supervision, Methodology, Investigation, Conceptualization.

Declaration of competing interest

The authors declare no conflicts of interest.

Acknowledgement

The genomic sequences and position of deletion were submitted to Genbank with accession numbers OR168074 and OR168075. We thank Dr. Phil F. Cruz (Red Bird Animal Clinic) for providing analysis of the samples of Wilfred Bachas-Daunert, an Italian greyhound, who likes to bask in the sun. Dr. Sylvia Daunert thanks the Miller School of Medicine of the University of Miami for the Lucille P. Markey Chair in Biochemistry and Molecular Biology.

Appendix A. Supplementary data

Supplementary data to this article can be found online at https://doi.org/10.1016/j.amolm.2024.100039.

References

Amos, W., Clarke, A., 2008. Body temperature predicts maximum microsatellite length in mammals. Biol. Lett. 4 (4), 399–401.
Ashour, M.E., Allam, W., Elsayed, W., Atteya, R., Elserafy, M., Magdeldin, S., Hassan, M. K., El-Khamisy, S.F., 2021. High temperature drives topoisomerase mediated chromosomal break repair pathway choice. Cancers 13 (10).
Belfield, E.J., Brown, C., Ding, Z.J., Chapman, L., Luo, M., Hinde, E., van Es, S.W., Johnson, S., Ning, Y., Zheng, S.J., Mithani, A., Harberd, N.P., 2021. Thermal stress accelerates Arabidopsis thaliana mutation rate. Genome Res. 31 (1), 40–50.
Bettaieb, A., Averill-Bates, D.A., 2015. Thermotolerance induced at a mild temperature of 40 degrees C alleviates heat shock-induced ER stress and apoptosis in HeLa cells. Biochim. Biophys. Acta 1853 (1), 52–62.
Burnett, T.A., Kaur, M., Polsky, L., Cerri, R.L.A., 2020. Rumen-reticular temperature during estrus and ovulation using automated activity monitors in dairy cows. Front. Vet. Sci. 7, 597512.
Candreva, E.C., Keszenman, D.J., Barrios, E., Gelos, U., Nunes, E., 1993. Mutagenicity induced by hyperthermia, hot mate infusion, and hot caffeine in Saccharomyces cerevisiae. Cancer Res. 53 (23), 5750–5753.
Chatterjee, N., Lin, Y., Santillan, B.A., Yotnda, P., Wilson, J.H., 2015. Environmental stress induces trinucleotide repeat mutagenesis in human cells. Proc. Natl. Acad. Sci. U. S. A. 112 (12), 3764–3769.
Chatterjee, N., Lin, Y., Yotnda, P., Wilson, J.H., 2016. Environmental stress induces trinucleotide repeat mutagenesis in human cells by alt-nonhomologous end joining repair. J. Mol. Biol. 428 (15), 2978–2980.
Chen, L.L., Sabripour, M., Wu, E.F., Prieto, V.G., Fuller, G.N., Frazier, M.L., 2005. A mutation-created novel intra-exonic pre-mRNA splice site causes constitutive activation of KIT in human gastrointestinal stromal tumors. Oncogene 24 (26), 4271–4280.

Christodoulou, J., Craig, H.J., Walker, D.C., Weaving, L.S., Pearson, C.E., McInnes, R.R., 2006. Deletion hotspot in the argininosuccinate lyase gene: association with topoisomerase II and DNA polymerase alpha sites. Hum. Mutat. 27 (11), 1065–1071.
Consortium, A.P.G., 2017. AACR project GENIE: powering precision medicine through an international Consortium. Cancer Discov. 7 (8), 818–831.
Corless, C.L., McGreevey, L., Town, A., Schroeder, A., Bainbridge, T., Harrell, P., Fletcher, J.A., Heinrich, M.C., 2004. KIT gene deletions at the intron 10-exon 11 boundary in GI stromal tumors. J. Mol. Diagn. 6 (4), 366–370.
de Nardi, A.B., Dos Santos Horta, R., Fonseca-Alves, C.E., de Paiva, F.N., Linhares, L.C. M., Firmo, B.F., Ruiz Sueiro, F.A., de Oliveira, K.D., Lourenco, S.V., De Francisco Strefezzi, R., Brunner, C.H.M., Rangel, M.M.M., Jark, P.C., Castro, J.L.C., Ubukata, R., Batschinski, K., Sobral, R.A., da Cruz, N.O., Nishiya, A.T., Fernandes, S. C., Dos Santos Cunha, S.C., Gerardi, D.G., Challoub, G.S.G., Biondi, L.R., Laufer-Amorim, R., de Oliveira Paes, P.R., Lavalle, G.E., Huppes, R.R., Grandi, F., de Carvalho Vasconcellos, C.H., Dos Anjos, D.S., Luzo, A.C.M., Matera, J.M., Vozdova, M., Dagli, M.L.Z., 2022. Diagnosis, prognosis and treatment of canine cutaneous and subcutaneous mast cell tumors. Cells 11 (4).
de Silva, C.M., Reid, R., 2003. Gastrointestinal stromal tumors (GIST): C-kit mutations, CD117 expression, differential diagnosis and targeted cancer therapy with Imatinib. Pathol. Oncol. Res. 9 (1), 13–19.
Dong, X., Chen, R., 2020. Understanding aberrant RNA splicing to facilitate cancer diagnosis and therapy. Oncogene 39 (11), 2231–2242.
Eagle, R.A., Enriquez, M., Grellet-Tinner, G., Perez-Huerta, A., Hu, D., Tutken, T., Montanari, S., Loyd, S.J., Ramirez, P., Tripati, A.K., Kohn, M.J., Cerling, T.E., Chiappe, L.M., Eiler, J.M., 2015. Isotopic ordering in eggshells reflects body temperatures and suggests differing thermophysiology in two Cretaceous dinosaurs. Nat. Commun. 6, 8296.
Ernst, B., Setayesh, T., Nersesyan, A., Kundi, M., Fenech, M., Bolognesi, C., Misik, M., Ghane, M., Mousavi, S.F., Knasmuller, S., 2021. Investigations concerning the impact of consumption of hot beverages on acute cytotoxic and genotoxic effects in oral mucosa cells. Sci. Rep. 11 (1), 23014.
Gamperl, S., Stefanzl, G., Willmann, M., Valent, P., Hadzijusufovic, E., 2021. In vitro effects of histamine receptor 1 antagonists on proliferation and histamine release in canine neoplastic mast cells. Vet. Med. Sci. 7 (1), 57–68.
Greenblatt, M.S., Grollman, A.P., Harris, C.C., 1996. Deletions and insertions in the p53 tumor suppressor gene in human cancers: confirmation of the DNA polymerase slippage/misalignment model. Cancer Res. 56 (9), 2130–2136.
Gueck, T., Aschenbach, J.R., Fuhrmann, H., 2002. Influence of vitamin E on mast cell mediator release. Vet. Dermatol. 13 (6), 301–305.
Hadzijusufovic, E., Peter, B., Herrmann, H., Rulicke, T., Cerny-Reiterer, S., Schuch, K., Kenner, L., Thaiwong, T., Yuzbasiyan-Gurkan, V., Pickl, W.F., Willmann, M., Valent, P., 2012. NI-1: a novel canine mastocytoma model for studying drug resistance and IgER-dependent mast cell activation. Allergy 67 (7), 858–868.
Huang, Y., Chen, H., Zhou, L., Li, G., Yi, D., Zhang, Y., Wu, Y., Liu, X., Wu, X., Song, Q., Liu, L., Yi, D., 2017. Association between green tea intake and risk of gastric cancer: a systematic review and dose-response meta-analysis of observational studies. Publ. Health Nutr. 20 (17), 3183–3192.
Incorvaia, L., Fanale, D., Vincenzi, B., De Luca, I., Bartolotta, T.V., Cannella, R., Pantuso, G., Cabibi, D., Russo, A., Bazan, V., Badalamenti, G., 2021. Type and gene location of kit mutations predict progression-free survival to first-line imatinib in gastrointestinal stromal tumors: a look into the exon. Cancers 13 (5).
Ito, D., Frantz, A.M., Modiano, J.F., 2014. Canine lymphoma as a comparative model for human non-Hodgkin lymphoma: recent progress and applications. Vet. Immunol. Immunopathol. 159 (3–4), 192–201.
Jorgensen, L.B., Orsted, M., Malte, H., Wang, T., Overgaard, J., 2022. Extreme escalation of heat failure rates in ectotherms with global warming. Nature 611 (7934), 93–98.
Kempna, P., Reiter, E., Arock, M., Azzi, A., Zingg, J.M., 2004. Inhibition of HMC-1 mast cell proliferation by vitamin E: involvement of the protein kinase B pathway. J. Biol. Chem. 279, 50700–50709.
Kiupel, M., Camus, M., 2019. Diagnosis and prognosis of canine cutaneous mast cell tumors. Vet Clin North Am Small Anim Pract 49 (5), 819–836.
Krawczak, M., Cooper, D.N., 1991. Gene deletions causing human genetic disease: mechanisms of mutagenesis and the role of the local DNA sequence environment. Hum. Genet. 86 (5), 425–441.
Krawczyk, P.M., Eppink, B., Essers, J., Stap, J., Rodermond, H., Odijk, H., Zelensky, A., van Bree, C., Stalpers, L.J., Buist, M.R., Soullie, T., Rens, J., Verhagen, H.J., O'Connor, M.J., Franken, N.A., Ten Hagen, T.L., Kanaar, R., Aten, J.A., 2011. Mild hyperthermia inhibits homologous recombination, induces BRCA2 degradation, and sensitizes cancer cells to poly (ADP-ribose) polymerase-1 inhibition. Proc. Natl. Acad. Sci. U. S. A. 108 (24), 9851–9856.
Kumar, S., Behl, T., Sachdeva, M., Sehgal, A., Kumari, S., Kumar, A., Kaur, G., Yadav, H. N., Bungau, S., 2021. Implicating the effect of ketogenic diet as a preventive measure to obesity and diabetes mellitus. Life Sci. 264, 118661.
Lasota, J., Jasinski, M., Sarlomo-Rikala, M., Miettinen, M., 1999. Mutations in exon 11 of c-Kit occur preferentially in malignant versus benign gastrointestinal stromal tumors and do not occur in leiomyomas or leiomyosarcomas. Am. J. Pathol. 154 (1), 53–60.
Lee, S.C., Dvinge, H., Kim, E., Cho, H., Micol, J.B., Chung, Y.R., Durham, B.H., Yoshimi, A., Kim, Y.J., Thomas, M., Lobry, C., Chen, C.W., Pastore, A., Taylor, J., Wang, X., Krivtsov, A., Armstrong, S.A., Palacino, J., Buonamici, S., Smith, P.G., Bradley, R.K., Abdel-Wahab, O., 2016. Modulation of splicing catalysis for therapeutic targeting of leukemia with mutations in genes encoding spliceosomal proteins. Nat. Med. 22 (6), 672–678.
Lees, A.M., Lees, J.C., Lisle, A.T., Sullivan, M.L., Gaughan, J.B., 2018. Effect of heat stress on rumen temperature of three breeds of cattle. Int. J. Biometeorol. 62 (2), 207–215.
Lees, A.M., Sejian, V., Lees, J.C., Sullivan, M.L., Lisle, A.T., Gaughan, J.B., 2019. Evaluating rumen temperature as an estimate of core body temperature in Angus feedlot cattle during summer. Int. J. Biometeorol. 63 (7), 939–947.
Lepock, J.R., 2005. How do cells respond to their thermal environment? Int. J. Hyperther. 21 (8), 681–687.
Letard, S., Yang, Y., Hanssens, K., Palmerini, F., Leventhal, P.S., Guery, S., Moussy, A., Kinet, J.P., Hermine, O., Dubreuil, P., 2008. Gain-of-function mutations in the extracellular domain of KIT are common in canine mast cell tumors. Mol. Cancer Res. 6 (7), 1137–1145.
Leung, A.K.C., Lam, J.M., Leong, K.F., 2019. Childhood solitary cutaneous mastocytoma: clinical manifestations, diagnosis, evaluation, and management. Curr. Pediatr. Rev. 15 (1), 42–46.
Levinson, G., Gutman, G.A., 1987. Slipped-strand mispairing: a major mechanism for DNA sequence evolution. Mol. Biol. Evol. 4 (3), 203–221.
Li, K., Wang, Z., 2021. Splicing factor SRSF2-centric gene regulation. Int. J. Biol. Sci. 17 (7), 1708–1715.
Li, Y., Yuan, Y., 2017. Alternative RNA splicing and gastric cancer. Mutat. Res. Rev. Mutat. Res. 773, 263–273.
Lin, Y., Zhang, X., Wang, Y., Zhang, J., Liu, Q., 2021. Single-stranded DNA generated by high temperature accepts protons and builds up mutagenic and carcinogenic strong acids. Mol. Biol. Rep. 48 (11), 7633–7635.
Loomis, D., Guyton, K.Z., Grosse, Y., Lauby-Secretan, B., El Ghissassi, F., Bouvard, V., Benbrahim-Tallaa, L., Guha, N., Mattock, H., Straif, K., G. International Agency for Research on Cancer Monograph Working, 2016. Carcinogenicity of drinking coffee, mate, and very hot beverages. Lancet Oncol. 17 (7), 877–878.
Masukume, G., Mmbaga, B.T., Dzamalala, C.P., Mlombe, Y.B., Finch, P., Nyakunga-Maro, G., Mremi, A., Middleton, D.R.S., Narh, C.T., Chasimpha, S.J.D., Abedi-Ardekani, B., Menya, D., Schuz, J., McCormack, V., 2022. A very-hot food and beverage thermal exposure index and esophageal cancer risk in Malawi and Tanzania: findings from the ESCCAPE case-control studies. Br. J. Cancer 127 (6), 1106–1115.
Molla, A., Block, M.R., 2000. Adherence of human erythroleukemia cells inhibits proliferation without inducing differentiation. Cell Growth Differ. 11 (2), 83–90.
Monteuuis, G., Schmitz, U., Petrova, V., Kearney, P.S., Rasko, J.E.J., 2021. Holding on to junk bonds: intron retention in cancer and therapy. Cancer Res. 81 (4), 779–789.
Montgomery, S.B., Goode, D.L., Kvikstad, E., Albers, C.A., Zhang, Z.D., Mu, X.J., Ananda, G., Howie, B., Karczewski, K.J., Smith, K.S., Anaya, V., Richardson, R., Davis, J., Genomes Project, C., MacArthur, D.G., Sidow, A., Duret, L., Gerstein, M., Makova, K.D., Marchini, J., McVean, G., Lunter, G., 2013. The origin, evolution, and functional impact of short insertion-deletion variants identified in 179 human genomes. Genome Res. 23 (5), 749–761.
Mullaney, J.M., Mills, R.E., Pittard, W.S., Devine, S.E., 2010. Small insertions and deletions (INDELs) in human genomes. Hum. Mol. Genet. 19 (R2), R131–R136.
Nakagawa, Y., Kajihara, A., Takahashi, A., Murata, A.S., Matsubayashi, M., Ito, S.S., Ota, I., Nakagawa, T., Hasegawa, M., Kirita, T., Ohnishi, T., Mori, E., 2018. BRCA2 protects mammalian cells from heat shock. Int. J. Hyperther. 34 (6), 795–801.
Nesta, A.V., Tafur, D., Beck, C.R., 2021. Hotspots of human mutation. Trends Genet. 37 (8), 717–729.
Oelkrug, R., Goetze, N., Exner, C., Lee, Y., Ganjam, G.K., Kutschke, M., Muller, S., Stohr, S., Tschop, M.H., Crichton, P.G., Heldmaier, G., Jastroch, M., Meyer, C.W., 2013. Brown fat in a protoendothermic mammal fuels eutherian evolution. Nat. Commun. 4, 2140.
Olivieri, F., 2020. Delta Tocotrienol and Melatonin in management of mast cell canine tumor Biomed. J Sci & Tech Res 28 (4), 21820–21822.
Orkin, M., 1967. Mastocytosis in animals. Arch. Dermatol. 96 (4), 381–385.
Ren, J.S., Freedman, N.D., Kamangar, F., Dawsey, S.M., Hollenbeck, A.R., Schatzkin, A., Abnet, C.C., 2010. Tea, coffee, carbonated soft drinks and upper gastrointestinal tract cancer risk in a large United States prospective cohort study. Eur. J. Cancer 46 (10), 1873–1881.
Richards, K.L., Suter, S.E., 2015. Man's best friend: what can pet dogs teach us about non-Hodgkin's lymphoma? Immunol. Rev. 263 (1), 173–191.
Robey, R.B., Hay, N., 2009. Is Akt the "Warburg kinase"?-Akt-energy metabolism interactions and oncogenesis. Semin. Cancer Biol. 19 (1), 25–31.
Roti Roti, J.L., 2008. Cellular responses to hyperthermia (40-46 degrees C): cell killing and molecular events. Int. J. Hyperther. 24 (1), 3–15.
Ruhle, A., Thomsen, A., Saffrich, R., Voglstatter, M., Bieber, B., Sprave, T., Wuchter, P., Vaupel, P., Huber, P.E., Grosu, A.L., Nicolay, N.H., 2020. Multipotent mesenchymal stromal cells are sensitive to thermic stress - potential implications for therapeutic hyperthermia. Int. J. Hyperther. 37 (1), 430–441.
Sette, C., Dolci, S., Geremia, R., Rossi, P., 2000. The role of stem cell factor and of alternative c-kit gene products in the establishment, maintenance and function of germ cells. Int. J. Dev. Biol. 44 (6), 599–608.
Seyfried, T.N., Mukherjee, P., Lee, D.C., Ta, L., Nations, L., 2023. Case report: resolution of malignant canine mast cell tumor using ketogenic metabolic therapy alone. Front. Nutr. 10, 1157517.
Sheikh, E., Tran, T., Vranic, S., Levy, A., Bonfil, R.D., 2022. Role and significance of c-KIT receptor tyrosine kinase in cancer: a review. Bosn. J. Basic Med. Sci. 22 (5), 683–698.
Spitzner, J.R., Muller, M.T., 1988. A consensus sequence for cleavage by vertebrate DNA topoisomerase II. Nucleic Acids Res. 16 (12), 5533–5556.
Spugnini, E.P., Vincenzi, B., Citro, G., Dotsinsky, I., Mudrov, T., Baldi, A., 2011. Evaluation of Cisplatin as an electrochemotherapy agent for the treatment of incompletely excised mast cell tumors in dogs. J. Vet. Intern. Med. 25 (2), 407–411.
Tang, Y.L., Fan, Y.L., Jiang, J., Li, K.D., Zheng, M., Chen, W., Ma, X.R., Geng, N., Chen, Q. M., Chen, Y., Liang, X.H., 2014. C-kit induces epithelial-mesenchymal transition and

contributes to salivary adenoid cystic cancer progression. Oncotarget 5 (6), 1491–1501.
Taniguchi, M., Nishida, T., Hirota, S., Isozaki, K., Ito, T., Nomura, T., Matsuda, H., Kitamura, Y., 1999. Effect of c-kit mutation on prognosis of gastrointestinal stromal tumors. Cancer Res. 59 (17), 4297–4300.
Taylor, M.S., Ponting, C.P., Copley, R.R., 2004. Occurrence and consequences of coding sequence insertions and deletions in Mammalian genomes. Genome Res. 14 (4), 555–566.
Thompson, J.J., Pearl, D.L., Yager, J.A., Best, S.J., Coomber, B.L., Foster, R.A., 2011a. Canine subcutaneous mast cell tumor: characterization and prognostic indices. Vet. Pathol. 48 (1), 156–168.
Thompson, J.J., Yager, J.A., Best, S.J., Pearl, D.L., Coomber, B.L., Torres, R.N., Kiupel, M., Foster, R.A., 2011b. Canine subcutaneous mast cell tumors: cellular proliferation and KIT expression as prognostic indices. Vet. Pathol. 48 (1), 169–181.
Treat, M.D., Scholer, L., Barrett, B., Khachatryan, A., McKenna, A.J., Reyes, T., Rezazadeh, A., Ronkon, C.F., Samora, D., Santamaria, J.F., Silva Rubio, C., Sutherland, E., Richardson, J., Lighton, J.R.B., van Breukelen, F., 2018. Extreme physiological plasticity in a hibernating basoendothermic mammal, Tenrec ecaudatus. J. Exp. Biol. 221 (Pt 20).
Tsuduki, T., Kuriyama, K., Nakagawa, K., Miyazawa, T., 2013. Tocotrienol (unsaturated vitamin E) suppresses degranulation of mast cells and reduces allergic dermatitis in mice. J. Oleo Sci. 62 (10), 825–834.
Turner, J.M., 2020. Facultative hyperthermia during a heatwave delays injurious dehydration of an arboreal marsupial. J. Exp. Biol. 223 (Pt 5).
Velichko, A.K., Petrova, N.V., Kantidze, O.L., Razin, S.V., 2012. Dual effect of heat shock on DNA replication and genome integrity. Mol. Biol. Cell 23 (17), 3450–3460.
Wang, B., Chen, L., Wang, W., 2019. Genomic insights into ruminant evolution: from past to future prospects. Zool. Res. 40 (6), 476–487.
Willmann, M., Hadzijusufovic, E., Hermine, O., Dacasto, M., Marconato, L., Bauer, K., Peter, B., Gamperl, S., Eisenwort, G., Jensen-Jarolim, E., Muller, M., Arock, M., Vail, D.M., Valent, P., 2019. Comparative oncology: the paradigmatic example of canine and human mast cell neoplasms. Vet. Comp. Oncol. 17 (1), 1–10.
Willmann, M., Yuzbasiyan-Gurkan, V., Marconato, L., Dacasto, M., Hadzijusufovic, E., Hermine, O., Sadovnik, I., Gamperl, S., Schneeweiss-Gleixner, M., Gleixner, K.V., Bohm, T., Peter, B., Eisenwort, G., Moriggl, R., Li, Z., Jawhar, M., Sotlar, K., Jensen-Jarolim, E., Sexl, V., Horny, H.P., Galli, S.J., Arock, M., Vail, D.M., Kiupel, M., Valent, P., 2021. Proposed diagnostic criteria and classification of canine mast cell neoplasms: a consensus proposal. Front. Vet. Sci. 8, 755258.
Wong, J.J., Au, A.Y., Ritchie, W., Rasko, J.E., 2016. Intron retention in mRNA: No longer nonsense: known and putative roles of intron retention in normal and disease biology. Bioessays 38 (1), 41–49.
Wong, J.J., Gao, D., Nguyen, T.V., Kwok, C.T., van Geldermalsen, M., Middleton, R., Pinello, N., Thoeng, A., Nagarajah, R., Holst, J., Ritchie, W., Rasko, J.E.J., 2017. Intron retention is regulated by altered MeCP2-mediated splicing factor recruitment. Nat. Commun. 8, 15134.
Wu, Z., Xue, S., Zheng, B., Ye, R., Xu, G., Zhang, S., Zeng, T., Zheng, W., Chen, C., 2019. Expression and significance of c-kit and epithelial-mesenchymal transition (EMT) molecules in thymic epithelial tumors (TETs). J. Thorac. Dis. 11 (11), 4602–4612.
Wu, J., Zhang, W., Li, C., 2020. Recent advances in genetic and epigenetic modulation of animal exposure to high temperature. Front. Genet. 11, 653.
Zingg, J.M., 2007. Vitamin E and Mast Cells. Academic Press.